

1. INTRODUCTION

The Quick Urban and Industrial Complex (QUIC) atmospheric dispersion modeling system attempts to fill an important gap between the fast, but non-building-aware Gaussian plume model and the building-aware but slow computational fluid dynamics (CFD) model. While Gaussian models have the ability to give answers quickly to emergency responders, they are unlikely to be able to adequately account for the effects of the building-induced complex flow patterns on the near-source dispersion of contaminants. QUIC uses a diagnostic mass-consistent empirical wind model called QUIC-URB that is based on the methodology of Röckle (1990). In this approach, the recirculation zones that form around and between buildings are inserted into the flow using empirical parameterizations and then the wind field is forced to be mass consistent. Although not as accurate as CFD codes, this approach is several orders of magnitude faster and accounts for the bulk effects of buildings.

In this paper, we discuss improvements recently made to the QUIC-URB wind model. These include modifications to the downwind cavity and upwind recirculation building flow parameterizations in QUIC-URB based on comparisons to wind-tunnel data which have shown that the original algorithms performed poorly for buildings with extreme aspect ratios. The building flow algorithms have also been modified so that they can account for buildings that are not aligned with one another, that is, buildings can now be rotated relative to the orthogonal grid system. As part of this upgrade, the way in which street canyon zones are determined was changed as well.

In addition, several new building types have been added to QUIC-URB including: a parking garage that allows air to pass through and outdoor stadiums of elliptical and rectangular shapes with open or partial roofs. In the sections that follow, we will provide an overview of the new building types and building parameterizations. An evaluation of the new and old algorithms against wind-tunnel data and computational fluid dynamics simulations will also be presented.

*Corresponding author address: Matthew A. Nelson, Los Alamos National Laboratory, P.O. Box 1663, MS K551, Los Alamos, NM 87545; e-mail: nelsonm@lanl.gov

2. MODIFICATIONS TO EXISTING ALGORITHMS

2.1 Downwind Cavity

In QUIC-URB the downwind cavity region is an ellipsoid extending downwind of the building (Fig. 1). The length of the ellipsoid region (L_r) is a function of the effective width (W_{eff}), effective length (L_{eff}), and height (H) of the building (Hosker 1984).

$$L_r = \frac{1.8W_{eff}}{(L_{eff}/H)^{0.03}(1+0.24W_{eff}/H)} \quad (1)$$

This formula was derived from wind-tunnel data for flow perpendicular to the building face. However, for flow that is oblique to the building face, it is not entirely clear how to apply Eq. 1. In the original algorithm L_{eff} and W_{eff} are defined by the maximum along-wind and cross-wind extents of the building, respectively (Fig. 1a). The ellipsoid extends from an imaginary surface at the maximum downwind distance of the building. For the case of perpendicular winds this surface is the downwind face of the building. For oblique winds, this surface touches the back corner of the building and is perpendicular to the wind direction (see Fig. 1a). In the modified algorithm L_{eff} and W_{eff} are defined as the maximum along-wind and cross-wind cross sections, respectively (Fig. 1b). In addition, the length of the ellipsoid region is measured from the downwind face(s).

The wind tunnel data of Snyder (2005) show that the downwind cavity region of wide buildings exhibits complex behavior under oblique winds. As the wind direction deviates from being perpendicular to the wide front face, the flow reattaches on the downwind side splitting the cavity in two (Fig. 2). Under these conditions the wide building is more streamlined and the flow patterns resemble those of a poorly-designed

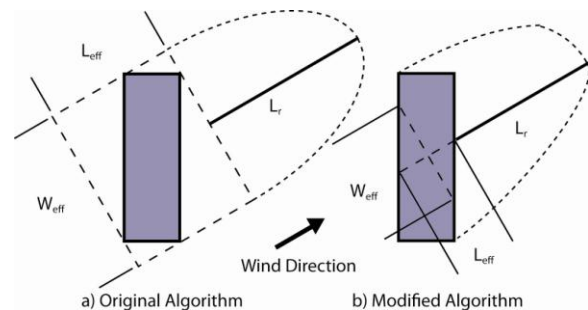


Figure 1 Schematics showing the parameters that are used to calculate the length of the ellipsoid region that defines the downwind cavity.

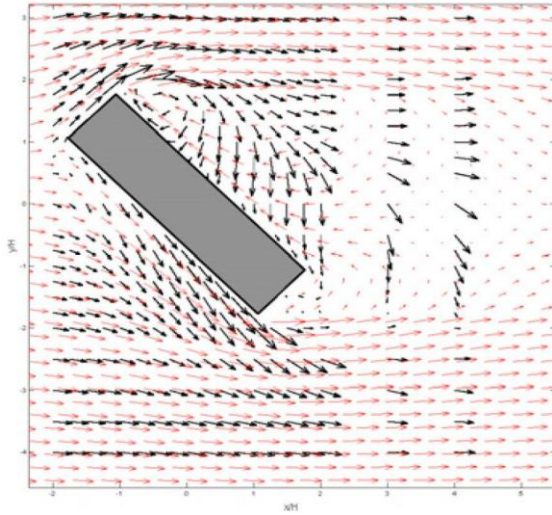


Figure 2 Comparison of the modeled winds from the original cavity algorithm and wind tunnel observations for flow around a rectangular building under winds rotated 45° from perpendicular to the wide side at $z \sim 0.1H$. The red vectors are from QUIC-URB and the black vectors are data from Snyder 2005.

airfoil with regions of flow separation. The comparison of the original cavity algorithm with the wind-tunnel data shown in Fig. 2 shows that instead of producing two small recirculation zones on the leading and trailing edges of the building the original algorithm places two large counter-rotating vortices in an overly large cavity zone behind the entire building.

The modeled wind field using the modified algorithm in Fig. 3 shows that the extent of the cavity region is significantly reduced yielding far better agreement with the observed wind field. In essence the original algorithm created a cavity zone as if the entire frontal area acted to block the flow as efficiently as a perpendicular face does. The new algorithm takes into account the streamlining effect that the oblique wind angles create. While the modified algorithm significantly improves the simulation of this flow, it does not reattach on the downwind face of the building as is shown in the measurements. In order to further improve the simulation of flow behind wide buildings under oblique winds a new algorithm that allows the cavity to be split will need to be developed.

The original algorithm for elliptical buildings is identical to the rectangular building algorithm. This causes two problems: first, for wind angles oblique to the orthogonal grid, the wakes extended out laterally as if the building were rectangular (not shown); second, since the algorithm was developed for rectangular buildings, the parameterization does not take into account the inherent streamlining of elliptical buildings and produces an L_r that is too large. Since the modified algorithm follows the downwind face of the building the first issue is resolved. To resolve the second issue the coefficient of 1.8 in the numerator of Eq. 1 is reduced to 0.9 for elliptical buildings. Fig. 4 is a comparison of near-surface streamlines around a

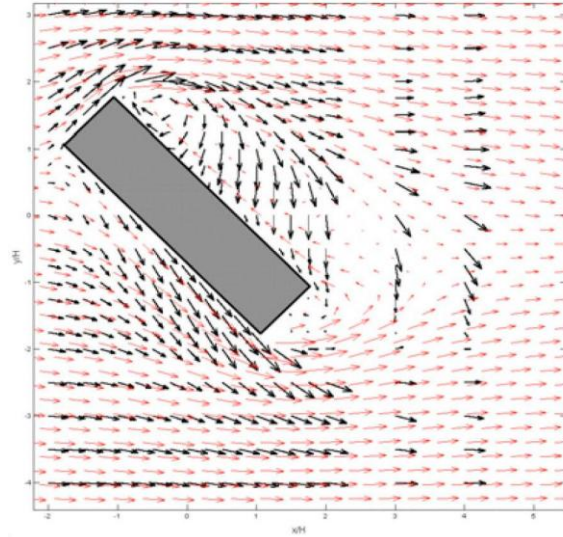


Figure 3 Comparison of the modeled winds from the modified cavity algorithm and wind tunnel observations for flow around a rectangular building under winds rotated 45° from perpendicular to the wide side at $z \sim 0.1H$. The red vectors are from QUIC-URB and the black vectors are data from Snyder 2005.

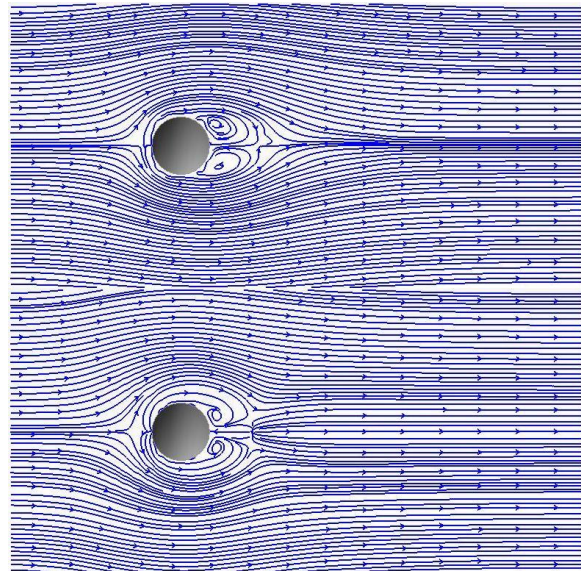


Figure 4 Comparison of simulations of flow around a cylinder with $H = 2D$ at $z \sim 0.05H$ by the modified algorithm in QUIC-URB (above) and QUIC-CFD (below).

cylindrical building with the diameter (D) is $0.5H$ as simulated by the modified QUIC algorithm and QUIC-CFD. QUIC-CFD was developed for speed and uses a simple turbulence model (Gowardhan et al. 2007). Fig. 4 shows that the new algorithm produces a comparable cavity region to that produced by QUIC-CFD. The original algorithm produces a cavity region that is twice as large (not shown).

2.2 Upwind Recirculation

When the wind direction is within 10° of being perpendicular to a building QUIC-URB places a vortex along the upwind face (Fig. 5). The region where the algorithm is applied is defined by an ellipsoid similar to the downwind cavity. The length of the ellipsoid (L_f) is a function of H and W (Hosker 1984).

$$L_f = \frac{1.5W}{1 + 0.8W/H} \quad (2)$$

The original algorithm used by Röckle(1990) and Kaplan and Dinar (1996) followed Hosker (1984) and multiplied W by 2 in the numerator instead of 1.5 and simply set all the velocities to zero within a single ellipsoid, relying on conservation of mass to produce the vortex in the region. Bagal et al. (2004) improved upon this simple algorithm by creating the Modified Vortex Parameterization (MVP) who changed the coefficient in the numerator to 1.5. MVP has two ellipsoid regions as is shown in Fig. 5. In the outer region velocities are reduced to 40% of their initial values and a vortex is placed in the inner region. Both ellipsoids extend up to $0.6H$.

A wind-tunnel investigation into this region by Addepalli and Pardyjak (2007) showed that the MVP algorithm does not adequately simulate the upwind recirculation region for tall buildings (see Fig. 6). Reducing all velocities by the same amount in the velocity deficit region incorrectly results in a sharp change in velocity at the boundary of the ellipsoid. While the upwind vortices produced by the MVP algorithm are approximately the right size for buildings with H/W near unity and below (not shown), the vortices on tall buildings are far too large (Fig. 6b). With these issues in mind, the high-rise MVP algorithm (HMVP) linearly reduces the velocities in the velocity deficit region from their upwind values at the outer surface to 40% of the initial values on the inner surface. HMVP also extends the vortex ellipsoid up to 60% of the minimum of H and W . These

modifications can be seen to smooth the transition between the ambient flow and the velocity deficit region and reduce the size of the vortex to better match the wind tunnel observations (Fig. 6c). The reason for the failure of the MVP for high-rise buildings is likely due to the fact that as H becomes much larger than W the upper region of the building acts more like a rectangular cylinder in cross flow than a surface mounted building. The building forces more of the flow around the sides rather than up and over the building.

2.3 Building Rotation

Since QUIC-URB uses an orthogonal grid there is a preferred orientation for the buildings. Previously buildings that were not aligned with this preferred orientation had to be constructed of several smaller buildings as is shown in the top of Fig. 7. This had the negative consequence of resulting in a cavity zone that was much too small, since the cavity scheme is applied to each of the individual buildings separately, rather than as a whole (recall that the cavity length is proportional to the width of the building).

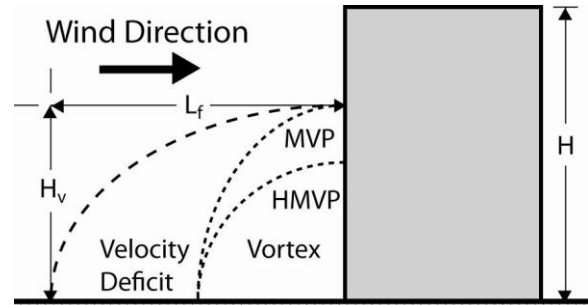


Figure 5 Schematic of the ellipsoid regions in the MVP and HMVP front recirculation algorithms.

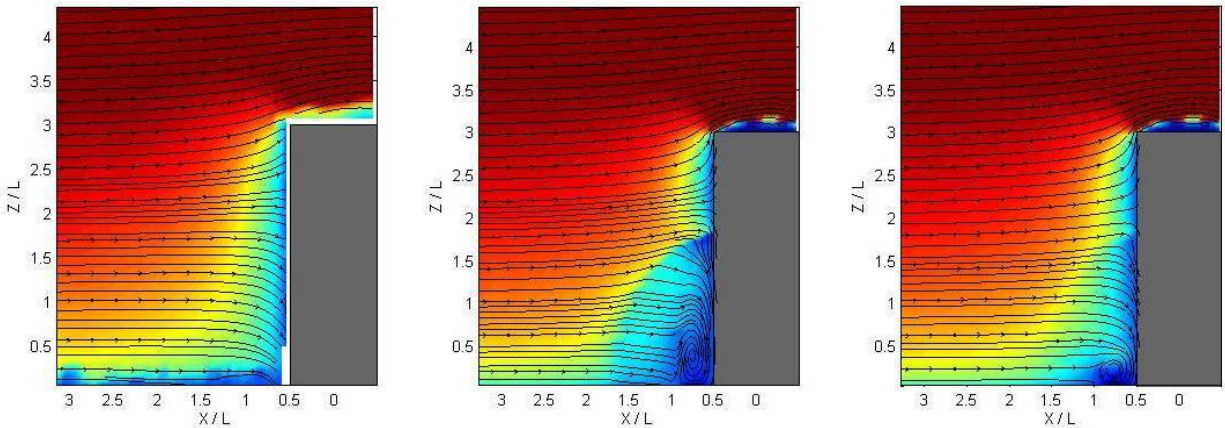


Figure 6 Comparison of the front recirculation on a building with $H/W = 3$ using wind-tunnel data (left), QUIC-URB using MVP (middle) and HMVP (right). Wind tunnel data obtained using particle image velocimetry in the University of Utah's Physical Fluid Dynamics Laboratory.

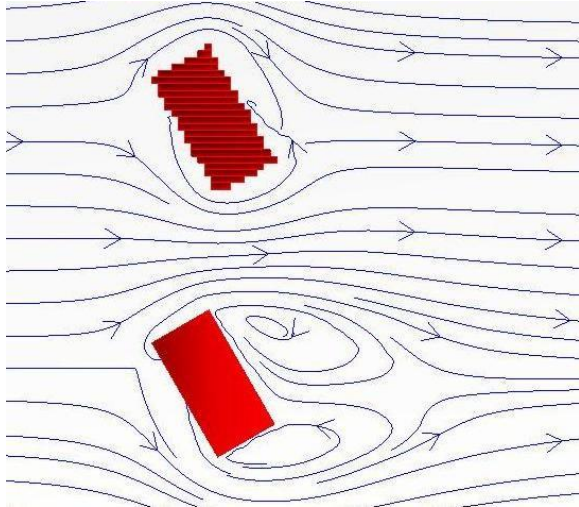


Figure 7 Comparison of the flow fields produced by a building created from slices (top) and created by specifying a building rotation angle (bottom).

QUIC-URB has been modified so that a rotation angle can be specified for each building. A non-aligned building can now be created from just one building. While the arrangements of solid and fluid cells are identical in the two ways of creating the rotated building due to the orthogonal grid, the two approaches give entirely different flow field patterns (Fig. 7). The new approach results in a much more reasonable larger-sized cavity zone due to using the correct width in the cavity length algorithm. The new approach also simplifies the construction of non-aligned buildings, significantly reducing the time to build a complex city. In order to implement building rotation, every one of the building flow algorithms had to be modified so that they could work in a rotated coordinate system.

2.4 Street Canyons with Building Rotation

The preferred orientation of the buildings in previous versions of QUIC-URB greatly simplified finding street canyons since they also had preferred orientations (Fig. 8). Allowing the buildings to rotate makes this process much more complex. Originally street canyons were placed anywhere the building separation distance to height ratio (S/H) ratio in the x and/or y directions was sufficiently small to be in the skimming flow regime as suggested by Oke (1987). Since there are no longer preferred directions, the new algorithm searches in the downwind direction a distance of L_r for other buildings. When a building is found within that distance a street canyon is formed along that plane up to the height of the lower of the two buildings (Fig. 8b).

3. NEW BUILDINGS

There are two basic building types in QUIC: rectangular and cylindrical. While complex building

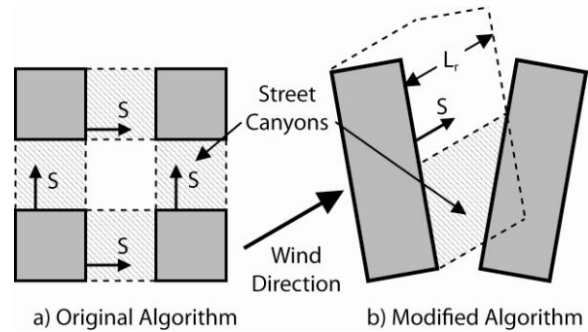


Figure 8 Schematics showing the methods used to determine street canyons with the original algorithm (a) and the building rotation algorithm (b). Dashed lines represent the areas where the algorithm searches for street canyons. The areas filled in with hashed lines represent the areas where the street canyon algorithm is applied.

geometries can be created by combining several simple buildings together, the resulting flow patterns may or may not simulate the behavior of the flow around the complex building. Fig. 7 shows that the best way to accurately simulate flow around a specific geometry is to use parameterizations specifically designed for that geometry. Recently new building types have been added to QUIC that are commonly found in urban areas: parking garages and stadiums.

3.1 Parking Garages

The parking garage building type is basically rectangular building that is partially permeable. The upwind and downwind cavity, street canyon, and rooftop flow algorithms are identical to the standard rectangular building. Internally the parking garage building is made of alternating slabs of fluid and solid cells. The velocities within the fluid cells in the interior are reduced from the upwind velocities by 50% (Schmidlin et al. 2004). The centerline cross section of the resulting flow is shown in Fig. 9. Due to the passage of air through the building, the front recirculation eddy and the cavity circulation are both weaker as compared to a solid building.

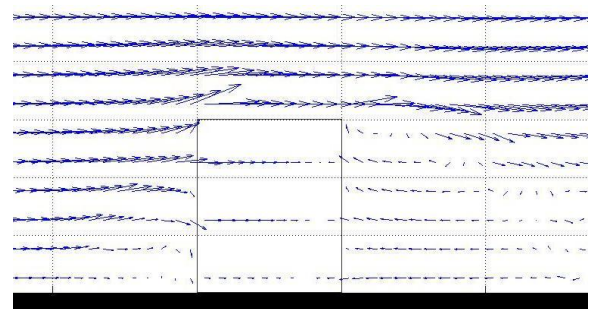


Figure 9 Centerline cross section of the flow in and around a parking garage building.

3.2 Stadiums

The primary difficulty in modeling stadiums is that while there are some basic shapes nearly every one is unique in some way. Since it is impossible to develop parameterizations for every distinct stadium, the parameterizations must be limited only to the basic designs. Currently there are four basic stadium shapes that have been added to QUIC (see Fig. 10): open elliptical, partial-roof elliptical, open rectangular, and partial-roof rectangular.

The courtyard of the stadiums is defined by the base wall thickness. The stadium wall thickness decreases linearly with height. Internally the stadium wall is always at least one grid cell to ensure that the wall is continuous. For open stadiums, the minimum wall thickness is at H . The minimum wall thickness occurs at $0.8H$ for partial-roof stadiums, above which is the roof. The opening in the roof has the same footprint as the opening in the base of the stadium.

The building flow parameterizations outside the stadium (e.g., downwind cavity, upwind rotor) are assumed to be identical to the corresponding standard building shapes. For the open stadiums a cavity ellipsoid extends from the upwind wall of the stadium with the same parameterization as is used in the downwind cavity region. For the partial-roof stadiums a vortex is placed under the awning on the upwind side of the stadium. The rest of the courtyard is left with the initial velocities. Most investigations into the flow around stadiums are concerned with surface pressures and wind loads (e.g., Barnard 2000 and Biagini et al. 2006). While this information is important for determining the safety of the structure in high winds, it is not particularly useful for parameterizing the flow in stadium courtyards. Therefore, in the absence of observed wind flow patterns QUIC-CFD was used to determine the flow patterns in the stadium courtyard. A comparison of the centerline streamlines for an open elliptical stadium produced by QUIC-CFD and QUIC-URB is shown in Fig. 11. The QUIC-CFD simulation shows a small region of separation at the top of the upwind wall with flow sweeping down into the courtyard

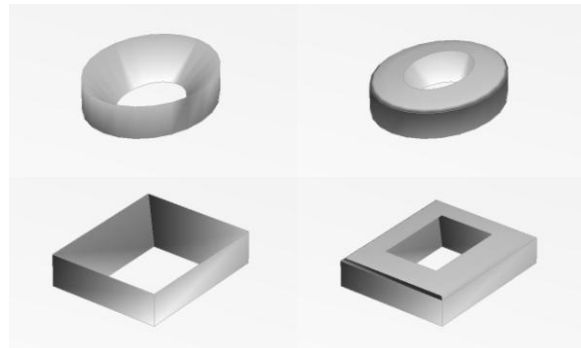


Figure 10 The four different types of stadium buildings in QUIC: open elliptical (upper left), partial-roof elliptical (upper right), open rectangular (lower left), and partial-roof rectangular (lower right).

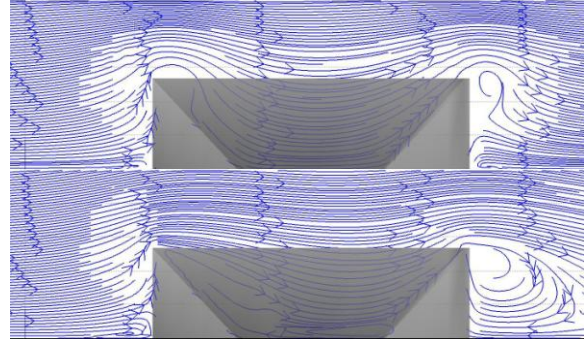


Figure 11 Centerline streamlines for flow around an open elliptical stadium as simulated by QUIC-CFD (above) and QUIC-URB (below).

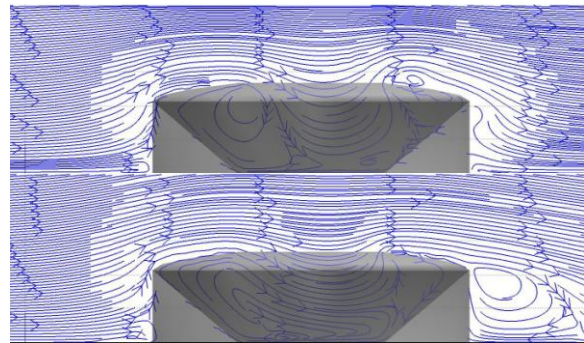


Figure 12 Centerline streamlines for flow around a partial-roof elliptical stadium as simulated by QUIC-CFD (above) and QUIC-URB (below).

interior and up the downwind wall. The QUIC-URB simulation has similar features but a larger cavity behind the upwind wall. A similar comparison but for a partial-roof elliptical stadium is presented in Fig. 12. The vortex appears to be stronger in the QUIC-CFD simulation but otherwise the two flow patterns look similar to each other.

4. CONCLUSIONS

Recent wind tunnel observations have shown that previous flow algorithms used in QUIC-URB did not adequately simulate the behavior for buildings with extreme aspect ratios. The downwind cavity algorithm was found to be far too large for wide buildings under oblique winds. The MVP front recirculation algorithm was found to produce vortices that were too large for high-rise buildings. Slight modifications to the existing algorithms improved performance in both instances. While the modifications to the downwind cavity algorithm significantly improved performance it did not accurately represent the splitting of the cavity. In order to simulate this behavior, major modifications to the algorithm are likely necessary.

The addition of building rotation greatly simplifies modeling buildings that are not aligned with the orthogonal grid used by QUIC. More importantly, creating a building from several smaller buildings

does not use the proper dimensions in the flow parameterizations. Many of the parameterizations are largely or entirely independent of other buildings, making the transition of these algorithms to a rotated coordinate system relatively straightforward. The street canyon algorithm, on the other hand, is dependent on the spacing between buildings. With rotated buildings this spacing may not be constant. The modified algorithm searches in planes aligned with the approach wind behind a building.

Flow around complicated building geometries is best simulated by parameterizing specifically for that geometry. Due to the fact that parking garages are common in urban areas and stadiums are thought to be high priority targets, these building types have been added to QUIC. Four stadium geometries were added: open elliptical, partial-roof elliptical, open rectangular, and partial-roof rectangular. In the absence of empirical data the stadium courtyard algorithms were developed using CFD simulations on the various stadium geometries. In addition, wind tunnel simulations of flow around stadiums are currently being conducted at the University of Utah that will be used to further refine the stadium flow algorithms.

5. REFERENCES

- Addepalli, B. and E.R. Pardyjak, 2007: *Personal communication*.
- Bagal, N., E.R. Pardyjak, and M.J. Brown, 2004: Improved upwind cavity parameterization for a fast response urban wind model. AMS 84th Annual Meeting: Symposium on Planning, Nowcasting, and Forecasting in the Urban Zone, P1.13, Seattle, WA, USA.
- Barnard, R.H., 2000: Predicting dynamic wind loading on cantilevered canopy roof structures. *J. Wind Eng. Ind. Aero.*, **85**, 47-57.
- Biagini, P., C. Borri, M. Majowiecki, M Orlando, and L. Procino, 2006: BLWT tests and design loads on the roof of the new Olympic stadium in Piraeus. *J. Wind Eng. Ind. Aero.*, **94**, 293-307.
- Gowardhan, A.A., E.R. Pardyjak, I. Senocak and M.J. Brown, 2007: A CFD based wind solver for a fast response dispersion model. Seventh Biennial Tri-Laboratory Engineering Conference, Albuquerque, New Mexico, May 7-10, 2007.
- Hosker, R.P., 1984: Flow and diffusion near obstacles. In *Atmospheric Power and Production*, SOE/TIG 27601.
- Kaplan, H. and N. Dinar, 1996: A Lagrangian dispersion model for calculating concentration distribution within a build-up domain. *Atmos. Environ.*, **30**, No. 24, 4197-4207.
- Oke, T.R., 1987: *Boundary Layer Climates*. London: Routledge, 2nd ed.
- Röckle R., 1990: Bestimmung der stomungsverhältnisse im bereich komplexer bebauungsstrukturen. Ph.D. thesis, Vom Fachbereich Mechanik, der Technischen Hochschule Darmstadt, Germany.
- Schmidlin, T.W., B. Hammer, L.S. Miller, G. Thumann, and H. Wetherington, 2004: Wind speeds in a parking garage during a hurricane and use of a parking garage as an evacuation refuge of last resort. AMS 26th Conference on Hurricanes and Tropical Meteorology, 11A.1, Miami, FL, U.S.A.
- Snyder, W.H., 2005: Streamline Patterns around Buildings Deduced from Wind-Tunnel Measurements. PHYSMOD, 2005, London, Ontario, Canada.